The 10th Asian Academic Society International Conference (AASIC)
GMPI Conference Series
Vol. 3, May 2024, pp. 34-43
ISSN: 2829-0747, DOI: 10.53889/gmpics.v3.419

Stress analysis of steam turbine rotor using Fluid-Structure Interaction simulation

Katanda Fajar Fauzi[1], Moch. Agus Choiron[2], Agung Sugeng Widodo[3], Yudy Surya Irawan[4], Djarot B. Darmadi[5], Anindito Purnowidodo[6]
[1,2,3,4,5,6] Brawijaya University, 10-11 Veteran Road, Malang, 65145, Indonesia

ARTICLE INFO

Article history:

Received January 10, 2024
Revised February 20, 2024
Published May 15, 2024

Keywords:

Steam Turbine;
Fluid-Structure Interaction (FSI);
Computational Fluid Dynamic (CFD);
Structural Simulation;
Stress Distribution

ABSTRACT

Steam Power Plant generates electricity due to a device that extracts heat energy from steam and converts it into mechanical work on the rotor. Turbines operate at high pressures and temperatures which may cause potential failures in the rotor. This study aims to determine the stress distribution on the turbine rotor to predict potential failures. The turbine studied is a 15 MW steam turbine with a rotation speed of 3000 rpm, inlet steam pressure of 2 MPa, and inlet steam temperature of 471.2 OC. The study focused on the Curtis stage. Fluid-Structure Interaction (FSI) simulation was performed to determine the interaction between the fluid and the turbine rotor. Computational Fluid Dynamic (CFD) was performed to determine the temperature and pressure hitting the rotor. The temperature and pressure distribution data from the CFD simulation is transferred to the structural simulation as the load received by the rotor. In addition to fluid loads, the rotor experiences centrifugal loads due to rotation and gravity loads. The largest stress received by the turbine rotor is at the front of the rotor with a stress of 347.39 MPa.

Corresponding Author:

Coresponding Author
Moch. Agus Choiron, Brawijaya University, 10-11 Veteran Road, Malang, 65145, Indonesia
Email: agus_choiron@ub.ac.id

1. INTRODUCTION

One of the plants used to meet electricity demand is the Steam Power Plant [1]. Steam Power Plants are capable of generating electricity due to the device that extracts heat energy from steam and converts it into mechanical work on the rotor [2]. Steam turbines operate at high pressures and temperatures that cause the rotor to be subjected to stress. Stresses lead to potential defects in the rotor [3]. Turbines are planned to operate for a certain period of time with calculated loading [4],[5]. However, when a defect occurs, the applied load remains the same. With a constant loading condition, the stress concentration occurs at the defect. This may lead to turbine rotor failure [6]. Rotor failures are devastating in terms of safety and economy [7]. The potential for failure can be reduced by performing periodic maintenance. Maintenance should focus on the parts with high stress distribution. Therefore, research to determine the stress distribution needs to be done. With the stress distribution data, maintenance can be focused on parts that have the potential for failure due to high stress. Experimental research using the real scale is difficult to do. The solution that can be used is to conduct research using the simulation method. The simulation used is Fluid-Structure Interaction (FSI) [8]. In this study, FSI is used to determine the structural response of the turbine rotor due to fluid interaction with the rotor. The known structural response will be the stress distribution that occurs in the rotor [9]. The data from the simulation is used for consideration of the possibility of failure. This is done to fulfill the long-term work plan. This study aims to determine the stress distribution in the curtis stage rotor of a 15 MW steam turbine with a rotation speed of 3000 rpm and an inlet steam temperature of 471.2 °C. The study started with geometry modeling, followed by FSI simulation. In the FSI simulation, Computational Fluid Dynamic (CFD) simulation is performed to determine the interaction of fluid with the structure, followed by structural simulation to determine the structural response in the form of stress distribution on the turbine rotor.

2. METHODS

The Curtis stage is the first stage of a multistage turbine. The Curtis stage consists of a nozzle followed by two rows of moving blades. After the water vapor passes through the curtis stage, the water vapor will go to the reaction stage. FSI analysis is performed on the curtis stage turbine rotor which consists of two stages of blades with 150 blades each. The specifications of the curtis stage rotor turbine are shown in Table 1. However, since the computational time required to complete the FSI simulation for the entire rotor is too large, the modeling is reduced to 1/30 of the entire rotor section as shown in Fig 1.

Table 1. Specifications of curtis stage steam turbine rotor

Parameter	Value	Unit
Rated power	15	MW
Number of blades	300	
Rotor radius	1188.5	mm
Rotor rotation speed	3000	rpm

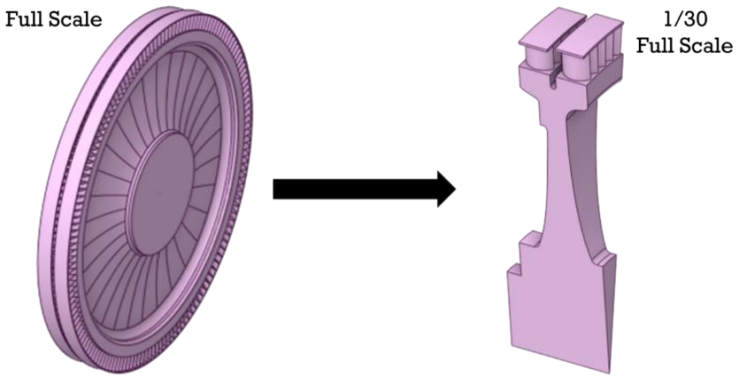

Fig 1. Full rotor modeling and reduction to 1/30

2.1. Computational Fluid Dynamics (CFD) Modeling

CFD investigations were performed on the turbine rotor to obtain the pressure and temperature values on the turbine rotor. Structural investigations on turbine rotors use CFD results at steady state as an input for structural simulations [10]. The reduced simulation is considered valid due to the cyclic periodicity of the flow in turbomachinery [11]. Thus, it is possible to analyze only a portion of the rotor with the application of periodic boundary conditions [12]. The geometry used in CFD is the negative domain of the rotor inside the steam turbine casing. The rotor geometry is later used for structural simulation. Fig 2 shows the geometry used for CFD simulation and structural simulation.

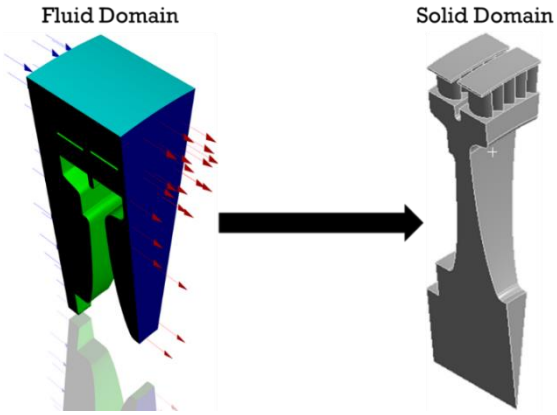

Fig 2. Fluid domain and solid domain

The domain and boundary conditions for the CFD simulation are shown in Fig 3. Water vapor with the properties listed in Table 2 enters through the turbine inlet with a pressure of 2 MPa and a temperature of 471.2 °C. After striking the blade, the vapor will exit the curtis stage and go to the reaction stage. The rotor is considered as a stationary non-slip wall, and a rotation frame is applied to the entire computational domain to account for the rotational speed of the rotor. This avoids the need for a dynamic mesh and allows problems

that are not essentially steady-state to be modeled using steady-state simulations, which significantly reduces computation time [13].

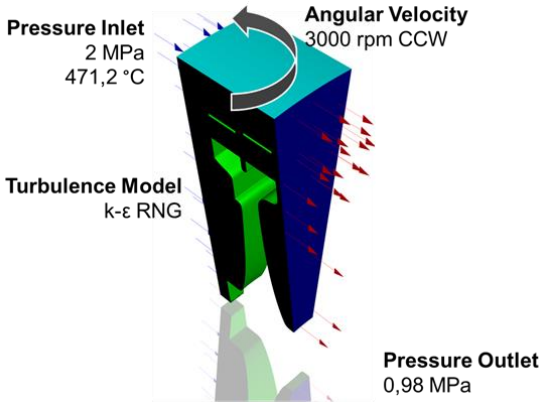

Fig 3. CFD Boundary condition

Table 2. Specifications of curtis stage steam turbine rotor

Parameter	Value	Unit
Density	0,5542	kg/m3
Specific heat (@ 471,2 °C)	2124	J/(kg K)
Thermal conductivity	0,0261	W/(m K)
Viscosity	1,34x10-5	kg/(m s)

To obtain accurate results for the flow domain is very important. The accuracy of the results and the number of elements must be well-balanced. The number of cells largely determines the efficiency of computational time [14]. Poly-Hexcore meshes show that the model is able to provide results that show good agreement between simulations and experiments [15]. The high-quality hexagon surface mesh shown in Fig 4 was prepared with ANSYS Fluent's proprietary meshing tool. The scoped sizing functionality was used to determine the size of the surface zones, based on curvature, proximity, and fine sizing requirements. This surface mesh was used to generate the Poly-Hexcore volume mesh shown in

Fig **5**. The mesh settings used produced the worst orthogonal quality with a value of 0.25 with a predicate of good.

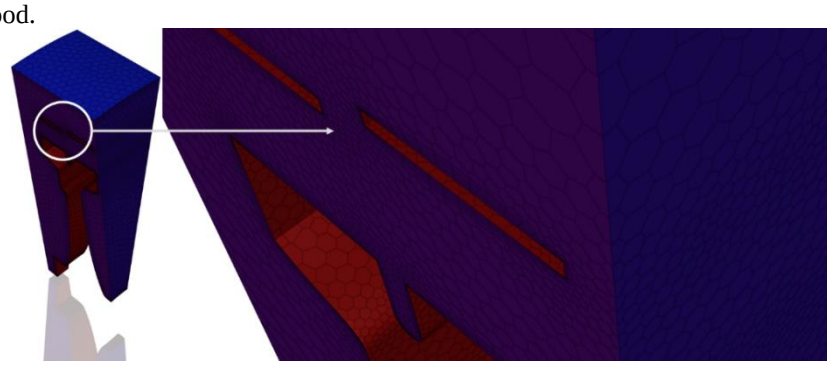

Fig 4. *Surface mesh*

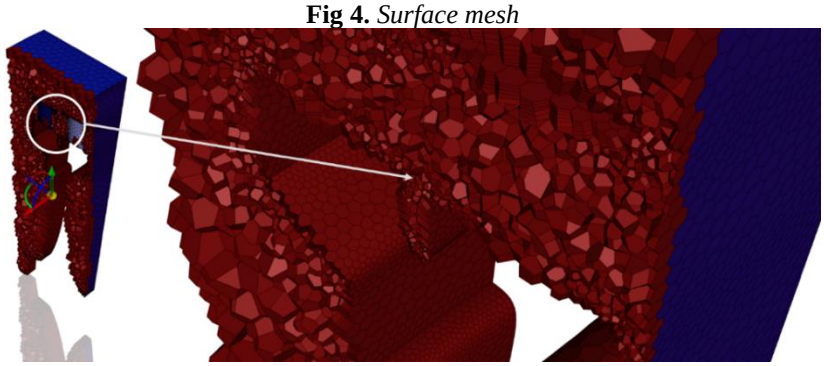

Fig 5. *Volume mesh*

In CFD simulations, the proposed RNG k-ε turbulence model [16] has several advantages when compared to the standard k-ε model, such as, significantly improving accuracy for strained flows, improving accuracy for rotating flows, and providing analytically derived differential formulas for low Reynolds number effects. However, the RNG k-ε model appears to require 10-15% more CPU time than the standard k-ε model due to additional terms and functions in the governing equations and a greater degree of nonlinearity (ANSYS, Inc., 2012). The fluid flow problem in this study is a nonlinear problem. Therefore, the solution of the problem is calculated iteratively. In this study, the number of iterations is set to 500, which is a relatively large number to ensure sufficient iterations to be performed. In addition, the standard initialization method is used, and the initial value is calculated from the inlet. After the solution is obtained, the results of CFD analysis, such as pressure and temperature distribution working on the rotor, can be displayed using the contour tool in ANSYS Fluent post-processing.

To assess the convergence of CFD analysis, the net mass imbalance is examined. The net mass imbalance of an analysis that is considered convergent should be less than 5% [17].

2.2. Static Structural Modeling

The material used for the rotor is structural steel with a density of 7850 (kg/m3). Detailed material properties are shown in Table 3.

Table 3. Material Properties

Temperature	Young's Modulus (GPa)	Yield Strenth (MPa)	Ultimate Tensil Strength (MPa)
20 °C	205	730	915
90 °C	200	736	924
150 °C	197	894	1122
205 °C	192	963	1209
260 °C	190	957	1201
316 °C	185	844	1060
371 °C	181	704	884
427 °C	176	543	681
482 °C	171	433	543
538 °C	165	279	350
593 °C	159	201	252

The meshing size is set with face sizing on the blade section with a size of 8 mm and body sizing on all parts of the rotor with a size of 8 mm (Fig 6). The mesh settings resulted in an average skewness of 0.25 with a very good predicate (ANSYS, Inc., 2012).

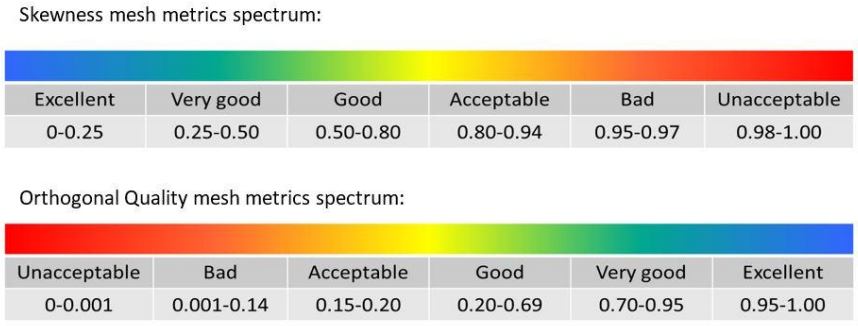

Fig 6. Mesh quality

The pressure and temperature from the CFD simulation are mapped on the rotor when performing the structural simulation. In addition to the fluid loads from the CFD simulation hitting the turbine rotor, there are other important loads on the rotor, namely 1) gravity loads, which are generated by the gravitational force acting on the turbine rotor; and 2) centrifugal loads, which are caused by the rotation of the turbine rotor. In

this study, the rotation speed is applied to the rotor structure to account for the centrifugal load and the gravity load is also applied to the turbine rotor structure as a static load. In addition, fixed boundary conditions are applied to the turbine shaft.

After defining the rotor geometry, material properties, mesh and boundary conditions, structural analysis can be performed. The results of the analysis in the form of stress distribution can then be displayed using the post-processing function of ANSYS software.

2.3. One-Way FSI Coupling

The coupling method in FSI modeling is based on one-way coupling. Fluid problems are solved using CFD. The pressure and temperature in all parts of the rotor obtained from CFD modeling are then mapped to the structural model as load boundary conditions. Afterwards, the structural model is used to calculate the structural response of the turbine rotor (stress distribution) under thermal, gravity, and centrifugal loads. The one-way FSI modeling scheme is presented in Fig 7.

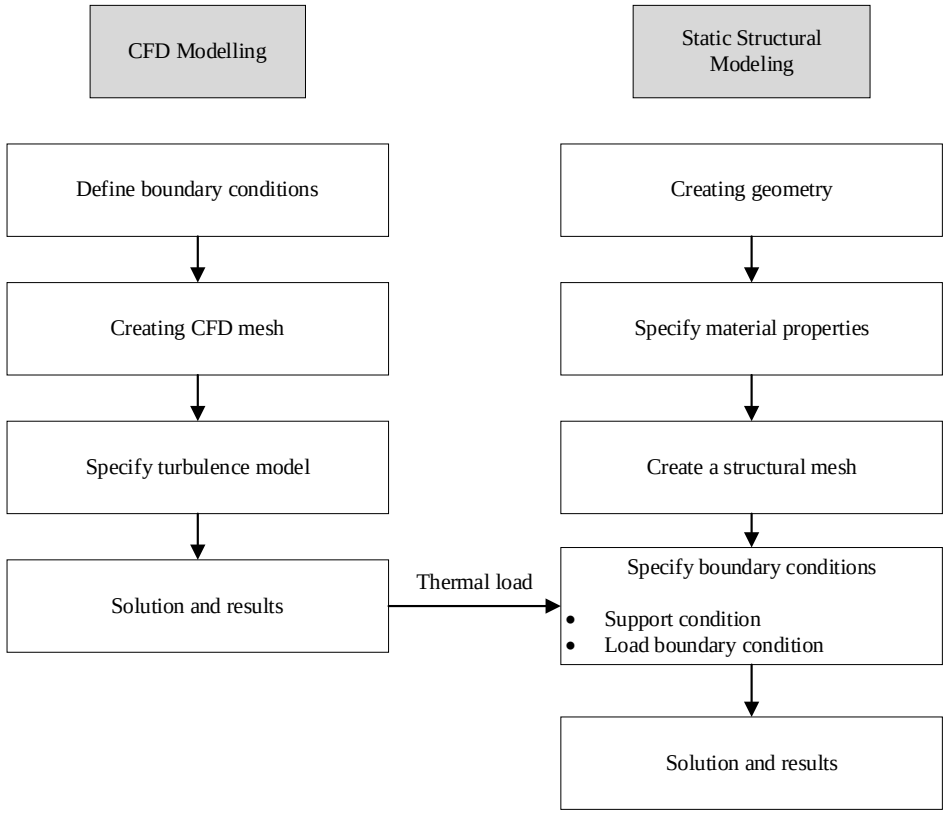

Fig 7. FSI scheme

3. RESULTS AND DISCUSSION

3.1. Pressure Distribution

Fig 8 shows the fluid pressure contours in the curtis zone. The left image shows the pressure contour in the curtis zone with an isometric view and the right image is a detailed image of the left image which is the pressure contour on the blade with a side view. Rainbow legend shows the pressure value in MPa. The color contours in the figure show the fluid flow pressure. Blue color indicates low fluid flow pressure, while red color indicates high fluid flow pressure.

Fluid flow with red contours on the wall close to the inlet indicates that the fluid flow pressure in that area is high. In blade 1 there is a color gradation from red at the first part of the blade that is exposed to fluid, then green in the middle of the blade, and orange at the back of the blade. The color gradation means that the fluid pressure changes when passing through blade 1. The gradation from red to green shows a pressure drop due to the expansion of the vapor due to the large potential energy possessed by the high-pressure water vapor entering the turbine casing. The gradation from green to orange shows that the water vapor experiences a slight increase in pressure due to water vapor that has lost its potential energy as it turns into kinetic energy that causes the turbine rotor to rotate. Then the water vapor exits blade 1 towards blade stage 2. When the steam

passes through blade 2, the same pressure change phenomenon occurs when the steam passes through blade 1 resulting in additional kinetic energy that allows the turbine rotor to rotate. From the figure, it can be seen that the fluid flow flows smoothly and regularly from the inlet to the curtis zone and then out to the reaction zone.

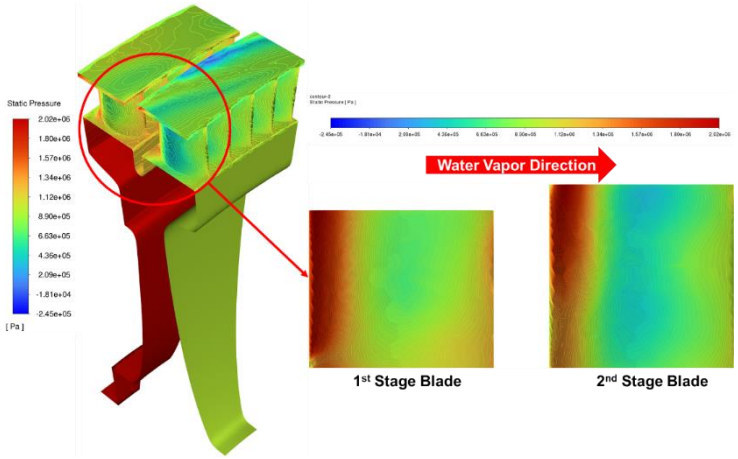

Fig 8. Pressure distribution

3.2. Temperature Distribution

Figure 9 shows the fluid temperature contours in the curtis zone. Rainbow legend shows the temperature value in °C. The color contours in the figure show the fluid flow temperature. Blue color indicates low fluid flow temperature, while red color indicates high fluid flow temperature.

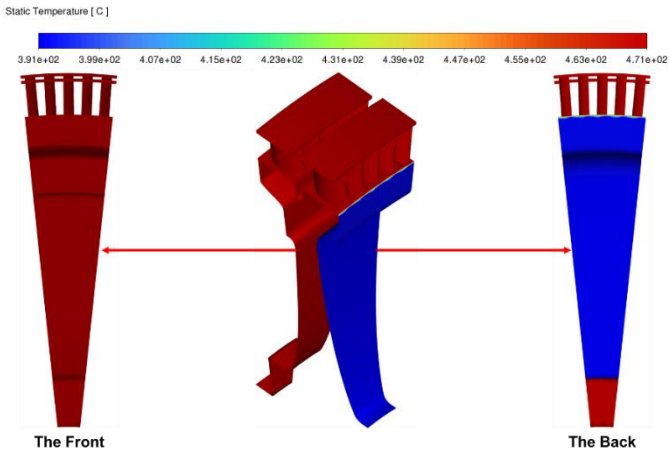

Fig 9. Temperature distribution

The fluid flow in almost all parts of the curtis zone is colored red, indicating that the fluid flow temperature in that section has the same temperature value of 471.2°C. The part that has a non-uniform temperature is the back of the stage 1 rotor with blue colored flow. This is due to the large water vapor pressure when entering the turbine casing which makes the water vapor that has passed through the blade flow directly to the reaction stage (Figure 10). From the figure, it can be seen that the fluid flow flows smoothly and regularly from the inlet to the curtis zone and then out to the reaction stage.

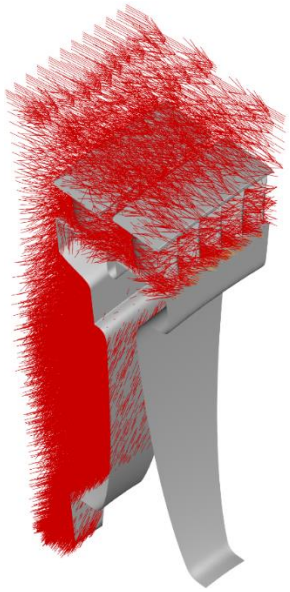

Fig 10. Water vapor fluid flow direction

3.3. Stress Distribution

Figure 11 shows the contours of the stress distribution (effective stress -von misses) in the curtis zone. Rainbow legend shows the stress value in MPa. The color contours in the figure indicates the stresses. The blue color indicates low stress, while the red color indicates high stress which means that the section is experiencing low stress. Overall, the rotor is dominated by blue and green colors. These color contours indicate that the stresses are low. However, there are some parts that have orange to red color contours. This color contour means that the stress is high. Parts that experience high stress are hubs which hold the blade as it acts as a support for the blade (Figure 12). Then the shaft, especially those with different diameters, also experiences high stress due to stress concentration (Figure 13).

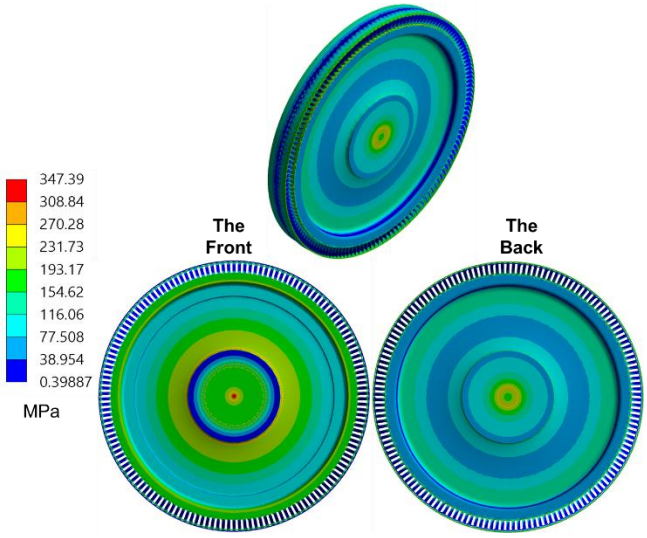

Fig 11. Stress distribution

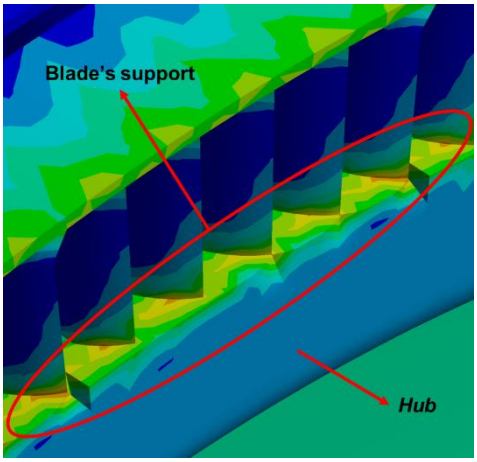

Fig 12. Stress on blade support

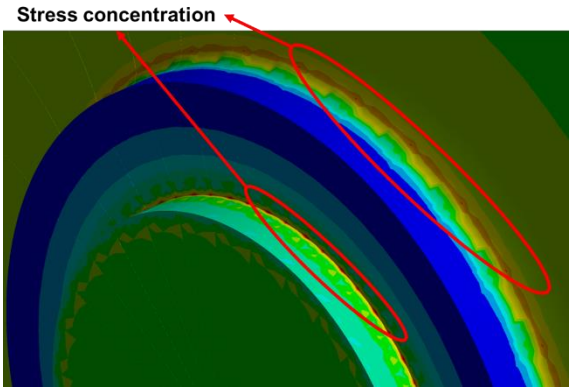

Fig 13. Stress concentration

Although there are some parts that experience high stress, the rotor has not yet failed as the working stress is still below the yield stress of the material. This is also evident from the safety factor value of the rotor in Fig 14, where the lowest value is 1.3068. The safety factor value above 1 means that the stress received by the rotor is still below the yield stress of the material. It will be risky if the stress is more than the yield stress or the safety factor value is below 1. If the safety factor value is below 1, it means that the rotor is plastically deformed. Starting with plastic deformation, cracks will appear and then lead to failure. Although the simulation results show a safety factor value above 1, this part needs more attention in the form of periodic checks and maintenance to avoid potential defects that lead to failure.

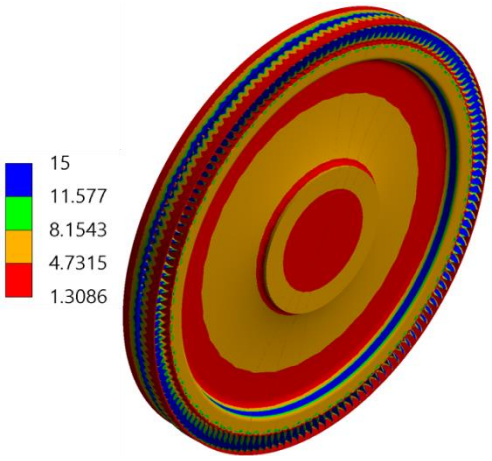

Fig 14. Safety factor value

4. CONCLUSION

In this study, an FSI model for a steam turbine rotor is created by combining CFD simulation and structural simulation. The coupling scheme is based on one-way coupling, where the load due to water vapor is calculated using CFD simulation and then mapped to the structural simulation as the load boundary condition. Then the FSI model is applied to the FSI modeling of the steam turbine rotor. The largest stress received by the turbine rotor is at the front of the rotor with a stress of 347.39 MPa. The high stress experienced by the front of the rotor is due to the high pressure and temperature of the water vapor hitting the front of the rotor. Although the stress received is high, the material has not yet failed as the working stress is still below the yield stress of the rotor material as evidenced by the safety factor value of the rotor where the lowest value is 1.3068. Although the simulation results show a safety factor value above 1, this part needs more attention in the form of periodic checks and maintenance to avoid potential defects that lead to failure.

ACKNOWLEDGMENTS

The authors express their gratitude to Brawijaya University's Design and Systems Engineering Laboratory for providing facilities for ANSYS research license. The Group Research Grant 2023 of the Faculty of Engineering, Brawijaya University, Indonesia provided funding for this study.

REFERENCES

[1] Hetharia, M., & Lewerissa, Y. J. (2018). Analisis Energi pada Perencanaan Pembangkit Listrik Tenaga Uap (PLTU) dengan Cycle Tempo. *Jurnal Voering*, *3*(1), 1–8.

[2] Toth, A., & Bobok, E. (2017). Geothermal Power Generation. In *Flow and Heat Transfer in Geothermal Systems* (pp. 243–273). Elsevier. https://doi.org/10.1016/B978-0-12-800277-3.00011-6.

[3] Banaszkiewicz, M. (2018). Numerical investigations of crack initiation in impulse steam turbine rotors subject to thermo-mechanical fatigue. Applied Thermal Engineering, 138, 761–773. https://doi.org/10.1016/j.applthermaleng.2018.04.099.

[4] Xiao, Y. Q., Liu, Z. Y., Zhu, W., & Peng, X. M. (2021). Reliability assessment and lifetime prediction of TBCs on gas turbine blades considering thermal mismatch and interfacial oxidation. Surface and Coatings Technology, 423. https://doi.org/10.1016/j.surfcoat.2021.127572.

[5] Ferreira, C., & Gonçalves, G. (2022). Remaining Useful Life prediction and challenges: A literature review on the use of Machine Learning Methods. *Journal of Manufacturing Systems*, *63*, 550–562. https://doi.org/10.1016/j.jmsy.2022.05.010.

[6] Fathyunes, L., & Mohtadi-Bonab, M. A. (2023). A Review on the Corrosion and Fatigue Failure of Gas Turbines. *Metals*, *13*(4). https://doi.org/10.3390/met13040701.

[7] Katinić, M., Kozak, D., Gelo, I., & Damjanović, D. (2019). Corrosion fatigue failure of steam turbine moving blades: A case study. *Engineering Failure Analysis*, *106*. https://doi.org/10.1016/j.engfailanal.2019.08.002.

[8] Marzec, Ł., Buliński, Z., & Krysiński, T. (2021). Fluid structure interaction analysis of the operating Savonius wind turbine. *Renewable Energy*, *164*, 272–284. https://doi.org/10.1016/j.renene.2020.08.145.

[9] Ubulom, I. (2021). Influence of fluid-structure interaction modelling on the stress and fatigue life evaluation of a gas turbine blade. *Proceedings of the Institution of Mechanical Engineers, Part A: Journal of Power and Energy*, *235*(5), 1019–1038. https://doi.org/10.1177/0957650920967559.

[10] Cai, L., He, Y., Wang, S., Li, Y., & Li, F. (2021). Thermal-fluid-solid coupling analysis on the temperature and thermal stress field of a nickel-base superalloy turbine blade. Materials, 14(12). https://doi.org/10.3390/ma14123315.

[11] Campobasso, M. S., & Giles, M. B. (2006). Stabilizing linear harmonic flow solvers for turbomachinery aeroelasicity with complex iterative algorithms. AIAA Journal, 44(5), 1048–1059. https://doi.org/10.2514/1.17069.

[12] Eltayesh, A., Hanna, M. B., Castellani, F., Huzayyin, A. S., El-Batsh, H. M., Burlando, M., & Becchetti, M. (2019). Effect of wind tunnel blockage on the performance of a horizontal axis wind turbine with different blade number. Energies, 12(10). https://doi.org/10.3390/en12101988.

[13] Wang, L., Quant, R., & Kolios, A. (2016). Fluid structure interaction modelling of horizontal-axis wind turbine blades based on CFD and FEA. Journal of Wind Engineering and Industrial Aerodynamics, 158, 11–25. https://doi.org/10.1016/j.jweia.2016.09.006.

[14] Arocena, V. M., & Danao, L. A. M. (2023). Improving the Modeling of Pressure Pulsation and Cavitation Prediction in a Double-Volute Double-Suction Pump Using Mosaic Meshing Technology. *Processes*, *11*(3). https://doi.org/10.3390/pr11030660.

[15] Karkoulias, D. G., Tzoganis, E. D., Panagiotopoulos, A. G., Acheimastos, S. G. D., & Margaris, D. P. (2022). Computational Fluid Dynamics Study of Wing in Air Flow and Air–Solid Flow Using Three Different Meshing Techniques and Comparison with Experimental Results in Wind Tunnel. *Computation*, *10*(3). https://doi.org/10.3390/computation10030034.

[16] Yakhot, V., Orszag, S. A., Thangam, S., Gatski, T. B., & Speziale, C. G. (1992). Development of turbulence models for shear flows by a double expansion technique. Physics of Fluids A, 4(7), 1510–1520. https://doi.org/10.1063/1.858424.

[17] Szabó, B., & Babuška, I. (2021). *Finite Element Analysis: Method, Verification and Validation* (2nd ed.). Wiley.

BIOGRAPHY OF AUTHORS

Katanda Fajar Fauzi, ST (katandaff@student.ub.ac.id)
He is a master student at Mechanical Engineering Department, Faculty of Engineering, University of Brawijaya, Malang, 65144, Indonesia.

Prof. Dr.Eng.Moch. Agus Choiron, ST., MT. (agus_choiron@ub.ac.id)
He is a professor at Mechanical Engineering Department, Faculty of Engineering, University of Brawijaya, Malang, 65144, Indonesia with specialization in design engineering optimization and computer simulation.

Agung Sugeng Widodo, ST., MT., Ph.D. (agung_sw@ub.ac.id)
He is an associate professor at Mechanical Engineering Department, Faculty of Engineering, University of Brawijaya, Malang, 65144, Indonesia with specialization in combustion, energy conversion, and energy alternatif.

Dr. Eng.Yudy Surya Irawan, ST., M. Eng. (yudysir@ub.ac.id)
He is an associate professor at Mechanical Engineering Department, Faculty of Engineering, University of Brawijaya, Malang, 65144, Indonesia with specialization in strength of materials, fracture & fatigue of materials, manufacturing process, and materials science.

Prof.Ir. Djarot B. Darmadi, MT., Ph.D. (b_darmadi_djarot@ub.ac.id)
He is a professor at Mechanical Engineering Department, Faculty of Engineering, University of Brawijaya, Malang, 65144, Indonesia with specialization in welding technologies and simulation.

Prof.Dr.Eng. Anindito Purnowidodo, ST., M.Eng. (anindito@ub.ac.id)
He is a professor at Mechanical Engineering Department, Faculty of Engineering, University of Brawijaya, Malang, 65144, Indonesia with specialization in strength of material, metal fatique, and crack behavior on engineering material.